

Mono- and di-nuclear Cu(II) complexes of *p*-*tert*-butyl-calix[4]arene-1,3-diacid derivative: A comparative study of their characterization and catecholase mimetic activity

Amjad Ali^a, Sunita Salunke-Gawali^a, Chebrolu P Rao^{a,*} & Jorge Linares^b

^aBioinorganic Laboratory, Department of Chemistry, Indian Institute of Technology Bombay, Mumbai 400 076, India
Email: cprao@chem.iitb.ac.in

^bLaboratoire de Magnétisme et d'Optique, CNRS-Université de Versailles, 78035 Versailles, France

Received 22 September 2005; revised 14 February 2006

Reaction of copper(II) perchlorate with *p*-*tert*-butyl-calix[4]arene-1,3-diacid gives mono-nuclear complex in acetonitrile and dinuclear complex in methanol which have been isolated as their pyridine bound adducts. The dinuclear complex exhibits different characteristics in its EPR and magnetic studies. The reactivity studies clearly indicate that the dinuclear complex has higher catecholase mimetic activity over its mononuclear counterpart owing to its coordination favourability.

IPC Code: Int. Cl.⁸ C07F1/08

Cu(II) based catecholase oxidases exhibit diverse physiological roles in various organisms, including in the biosynthesis of catecholamine neurotransmitters and hormones (dopamine, noradrenaline, adrenaline) of humans and vertebrates, as well as in the formation of pigment melanin and browning of cut fruits and vegetables¹⁻⁶. The catalytic mechanism of dinuclear copper complexes has been dealt with by Solomon *et al.*⁷ Studies reporting such activity of the copper complexes of calixarene derivatives are few⁸, and to our knowledge, no such study is reported with the calix[4]arene-di-acid derivative. In this paper, we report the synthesis and characterization of mono- and di-copper complexes of calix[4]arene-1,3-diacid and compare their characterization features and catecholase mimetic activities. The present study is a continuation of our recent efforts in metallo-chemistry of calix[4]arene derivatives⁸⁻¹¹.

Materials and Methods

p-*tert*-Butylphenol, formaldehyde and ethyl bromoacetate were procured from Lancaster (UK) and 3, 5-di-*tert*-butyl-catechol and Cu(ClO₄)₂·6H₂O from Sigma Chemicals. All solvents were purchased from local sources and were purified and dried by standard methods immediately before use. *p*-*tert*-Butyl-calix[4]arene-1,3-diacid (H₄L) was synthesized as reported earlier¹⁰.

Elemental analysis was carried out on Carlo Erba instruments Flash EA 1112 series/ThermoQuest EA 1112 and metal contents were determined by inductively coupled plasma atomic emission spectroscopy (ICP-AES). FTIR spectra were recorded in KBr matrix between 400 and 4000 cm⁻¹ on a Nicolet impact 400. UV-vis spectrophotometric experiments were performed on a Shimadzu UV-2101PC. The FAB mass spectra were recorded on a Jeol SX 102/DA-6000 mass spectrometer data system using argon/xenon (6 kV, 10 mA) as the FAB gas. The accelerating voltage was 10 kV and the spectra were recorded at room temperature using *m*-nitrobenzyl alcohol (NBA) as the matrix. Solution conductivity was measured using a Systronic conductivity bridge-302. The EPR spectra were recorded on a Varian (model 109C) E-line X-band spectrometer fitted with a quartz Dewar for measurements at 77K and calibrated by using tetracyanoethylene (TCNE, *g* = 2.00277). The magnetization curves were recorded using the SQUID magnetometer (Quantum Design MPMS5) and TGA and DTA were recorded on Shimadzu-thermal analyzer (DT-30).

Synthesis of complexes

[Cu(H₄L)₂Py], (I)

H₄L (100 mg, 0.133 mmol) was dissolved in CH₃CN and to this was added a solution of

$\text{Cu}(\text{ClO}_4)_2 \cdot 6\text{H}_2\text{O}$ (76 mg, 0.133 mmol) to give a clear light green solution which turns to yellow after one hour. To this solution, 0.25 mL of pyridine was added to give a light green precipitate. The reaction mixture was stirred for 12 hr to obtain a blue precipitate, which was washed with CH_3CN and then dried under vacuum. Yield: (60 mg) 54%; m.pt. 230°C (decomp.); $\text{C}_{101}\text{H}_{121}\text{NO}_{16}\text{Cu}$ (1668.58): C 72.70, H 7.31, N 0.84, Cu 3.81; found: C 72.56, H 7.11, N 1.07, Cu 3.64%. FTIR: (KBr, cm^{-1}): 1604, 1736 ($\nu_{\text{C}=\text{O}}$), 3410 (ν_{OH}). UV-vis: ($\lambda_{\text{max}}/\text{nm}$, $\epsilon/\text{dm}^3\text{mol}^{-1}\text{cm}^{-1}$): 282 (17030), 244 (20600), 677 (10). FAB-MS: m/z (intensity (%), fragment) 1596 (10, $[\{\text{Cu}(\text{H}_2\text{L})_2\} + \text{Li}]^+$); 825 (20, $[\{\text{Cu}(\text{H}_2\text{L})\} - 2\text{H}]^+$); 787 (100, $[\text{H}_4\text{L} + \text{Na}]^+$). Weight loss observed (13%) in TGA in the temperature range $100\text{--}170^\circ\text{C}$ is assignable to the loss of pyridine and CH_3CN .

$\{\text{Cu}(\text{H}_2\text{L})\text{Py}\}_2$ (**2**)

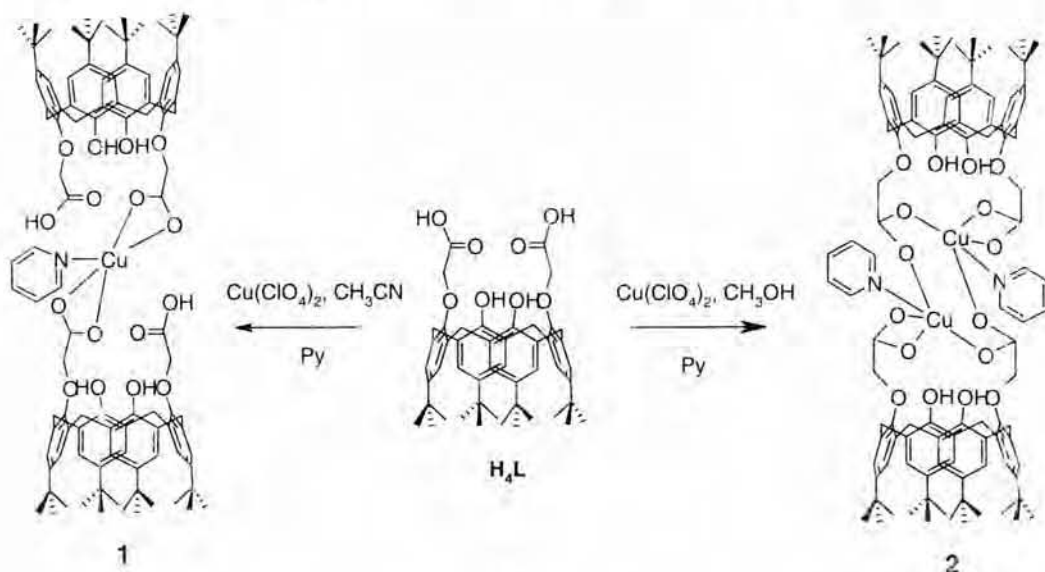
Complex **2** was prepared by the same method as that given for **1**, but using MeOH instead of CH_3CN . Yield: (79 mg) 65%; m.pt. $>220^\circ\text{C}$ (decomp.); $\text{C}_{53}\text{H}_{63}\text{NO}_8\text{Cu} \cdot \text{CH}_3\text{OH}$ (936.41): C 69.17, H 7.20, N 1.49, Cu 6.78; Found: C 68.94, H 6.83, N 1.35, Cu 6.92%. FTIR: (KBr, cm^{-1}): 1608, 1638 ($\nu_{\text{C}=\text{O}}$), 3403 (ν_{OH}). UV-vis ($\lambda_{\text{max}}/\text{nm}$, $\epsilon/\text{dm}^3\text{mol}^{-1}\text{cm}^{-1}$): 282 (32860), 249 (28960), 780 (6). FAB-MS: m/z (intensity (%), fragment) 1652 (4, $[\{\text{Cu}(\text{H}_2\text{L})_2\}^+]$); 827 (50, $[\text{Cu}(\text{H}_2\text{L})]^+$); 787 (32, $[\text{H}_4\text{L} + \text{Na}]^+$). Weight loss observed (5%) in TGA in the temperature range $60\text{--}165^\circ\text{C}$ is assignable to the loss of pyridine.

Results and Discussion

The reaction of *p-tert*-butyl-calix[4]arene-1,3-diacid (H_4L) with $\text{Cu}(\text{ClO}_4)_2 \cdot 6\text{H}_2\text{O}$ yielded a mono-nuclear complex **1** when carried out in CH_3CN and a dinuclear complex, **2** when carried out in CH_3OH , as shown in Scheme 1. Both **1** and **2** were characterized by elemental analysis, conductivity, VT magnetic susceptibility, TGA, FAB mass, FT-IR, UV-visible and VT EPR. The elemental analysis including that of the metal ion content fits well with a composition of metal to the ligand to pyridine ratio of 1:2:1 and 1:1:1 in **1** and **2** respectively. The molecular ion peaks observed in the FAB mass spectra were consistent with mono-nuclear in **1** and dinuclear in **2** and the spectra exhibit several other interpretable fragments as given under the experimental section. The presence of bound pyridine in both the complexes has been quantitatively demonstrated based on the weight loss observed in TGA under N_2 atmosphere in the temperature range $60\text{--}200^\circ\text{C}$. These complexes were found to be neutral based on the conductivity studies. Thus, the analytical data along with the mass spectral data fits well with the formula, $\{\text{Cu}(\text{H}_2\text{L})\text{Py}\}$ for **1** and $\{\text{Cu}(\text{H}_2\text{L})\text{Py}\}_2$ for **2**.

FTIR and UV-vis spectral studies

FTIR spectra of ligand shows a sharp band at 1747 cm^{-1} due to carboxylate vibration and this shifts to 1632 and 1607 cm^{-1} in **1** and **2** respectively upon Cu(II) binding. Besides, these complexes exhibited $\nu_{\text{s}}(\text{COO})$ at ~ 1480 and $\sim 1380\text{ cm}^{-1}$. The difference $\Delta\nu$



Scheme 1

($\nu_{\text{as(COO)}} - \nu_{\text{s(COO)}}$), viz., $\sim 120 \text{ cm}^{-1}$ and $\sim 220 \text{ cm}^{-1}$ are indicative of the coordination arising from monodentate and also from bidentate including bridging mode for the carboxylate groups in these complexes. These results agree well with the literature reports¹². Absorption spectra for **1** and **2** exhibit $d \rightarrow d$ transition at 677 and 780 nm, respectively, besides the ligand based ones, supporting the formation of Cu(II) complexes.

EPR spectral studies

The EPR spectra for **1** and **2** measured at 77K in its powder and glassy (CHCl_3) forms, exhibit characteristic differences between these two types of complexes as shown in Fig. 1. Mononuclear complex exhibits a spectrum that is typical of tetragonally elongated Cu(II) with $g_{\parallel} > g_{\perp} > 2$ and a $d_{x^2-y^2}$ ground state doublet¹³. The dinuclear complex **2** shows rhombic signal with resolved hyperfine splitting with $g_1 = 2.28$, $g_2 = 2.13$ and $g_3 = 1.98$ with $A_{\text{av}} = 48 \text{ G}$. No half-field signal was detected in **2**.

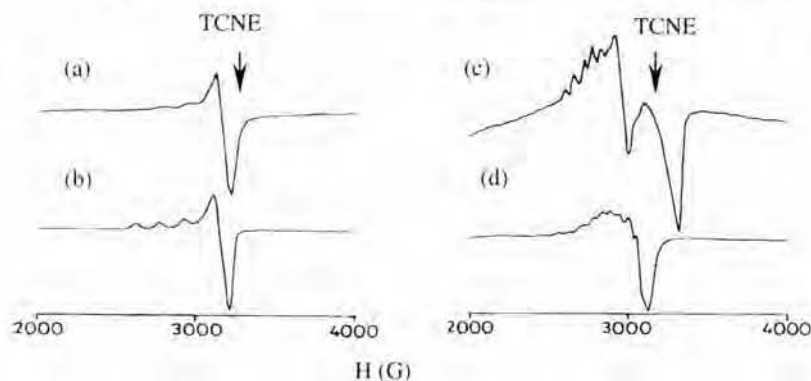


Fig. 1—EPR spectra of mono- and dinuclear complexes at 77 K. [(a) **1**, powder; (b) **1**, CHCl_3 ; (c) **2**, powder; (d) **2**, CHCl_3].

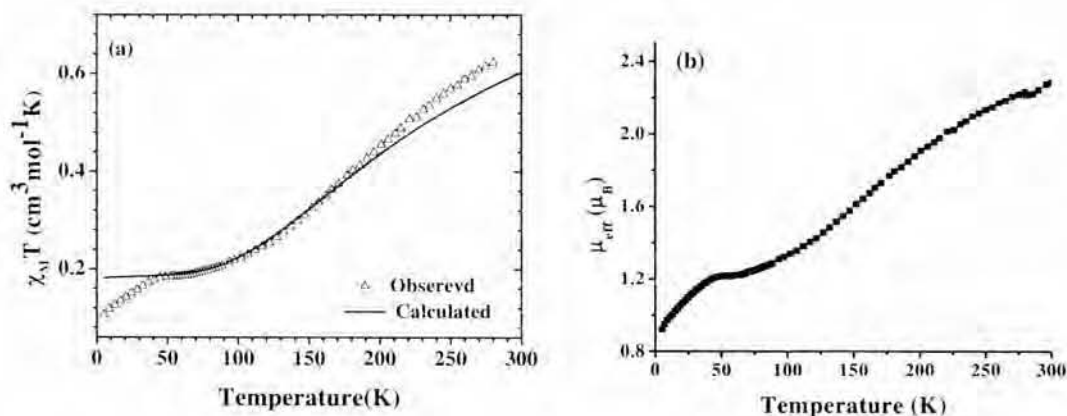


Fig. 2—(a) Plot of temperature vs $\chi_M T$ for **2** and (b) Plot of μ_{eff} vs T for **2**.

VTMS analysis

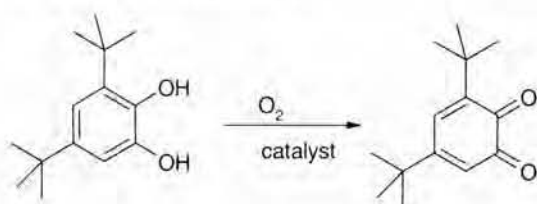
Plots of $\chi_M T$ versus T and μ_{eff} versus T are shown in Fig. 2 for complex **2**. The $\chi_M T$ plot was found to be $0.66 \text{ cm}^3 \text{ mol}^{-1} \text{ K}$ with $\mu_{\text{eff}} = 2.28 \mu_B$ at 300K which is less than that observed for two non-coupled Cu(II) centers. The $\chi_M T$ continuously decreases on cooling down to 75 K and exhibits a well-defined local maximum in the temperature range 75-45 K. A further decrease was observed in $\chi_M T$ up to 5 K where the value was found to be $0.10 \text{ cm}^3 \text{ mol}^{-1} \text{ K}$. The observed μ_{eff} varies from 2.28 to $0.92 \mu_B$ on going from 300 to 5K. This behaviour observed with **2** accounts for the antiferromagnetic coupling between the two copper (II) centers, extending to both intra- as well as inter-molecular types^{14,15}.

A best fit for the data was obtained only when paramagnetic impurity was introduced as shown by the expression, $\chi_M = (2Ng^2\beta^2/kT)[3+\exp(-J/kT)]^{-1}(1-p) + [Ng^2\beta^2/2kT]p + N\alpha$, where different terms present in this equation carry same meaning as that given in

the literature¹⁶. The fitting yields, $J = -315 \text{ cm}^{-1}$, $g = 2.2$, $p = 0.20$, $N\alpha = 0.000120$ and $R = 8.12 \times 10^{-5}$. Owing to the presence of large paramagnetic impurity in the complex, the synthesis was repeated at least five times and also the VT-magnetic susceptibility measurements. However, same result was obtained with several scannings. The value of $p = 0.20$ can also be accounted for based on the intermolecular interactions between the dimeric units of **2**, as that reported in the literature¹⁴.

Catecholase-mimetic activity of **1** and **2**

A general reaction for the catecholase mimetic activity is shown in Scheme 2.



The catecholase-mimetic activity studies were carried out in methanolic solution since the substrate, 3,5-di-*tert*-butylcatechol (3,5-DTBC) and the product, 3,5-di-*tert*-butyl-*o*-quinone (3,5-DTBQ) were soluble, and further the solutions of **1** and **2** in chloroform can be diluted with methanol. For the purpose of this study, a $6.25 \times 10^{-5} \text{ M}$ solution of **1** or **2**, in $\text{CHCl}_3/\text{MeOH}$ (7/93, v/v) were mixed with equal volume of $3.125 \times 10^{-3} \text{ M}$ solution of 3,5-DTBC (1:50

of **1** or **2** versus 3,5-DTBC). The course of the reaction was followed by measuring absorption spectra over a period of 16 hr and by monitoring the OD of 400 nm band that appears due to the formation of 3, 5-DTBQ as shown in Fig. 3. Initial rate of the reaction was derived from the plot of the OD of the 400 nm band versus time in both the cases. Similarly, the rate constant in both the cases was determined from the plot of $\ln(A_0 - A_\infty)/A_1 - A_\infty$ versus time as the reaction follows pseudo first order. In order to determine the kinetic parameters, the Michaelis-Menten approach was adapted¹⁷. For the determination of the kinetic parameters of **1** and **2**, the substrate concentrations were used at 3.125×10^{-4} , 6.25×10^{-4} and $1.563 \times 10^{-3} \text{ M}$ with fixed complex concentration of $3.125 \times 10^{-5} \text{ M}$. Figure 4 shows the Lineweaver-Burk plot obtained from these experiments and all the kinetic parameters calculated from these plots are summarized in Table 1. From the table it is evident that the binding of the substrate is better at least by about six times and that of the K_{cat} is better by at least two times in case of the di-nuclear copper complex (**2**) as compared to the mono-nuclear (**1**) owing to its bridged Cu_2O_2 core. The values obtained for dinuclear complexes in the literature¹⁵, viz., $K_M = 2.92 \times 10^{-3} \text{ M}$, $k_{\text{cat}} = 3.28 \times 10^{-2} \text{ s}^{-1}$, and $K_M/k_{\text{cat}} = 89.02 \times 10^{-3} \text{ Ms}$ were in the same order of magnitude as that found in case of the present dinuclear complex¹⁸. However, the enzymatic rate for catechol conversion in sweet potatoes¹⁹ has been measured to be $2.3 \times 10^3 \text{ s}^{-1}$.

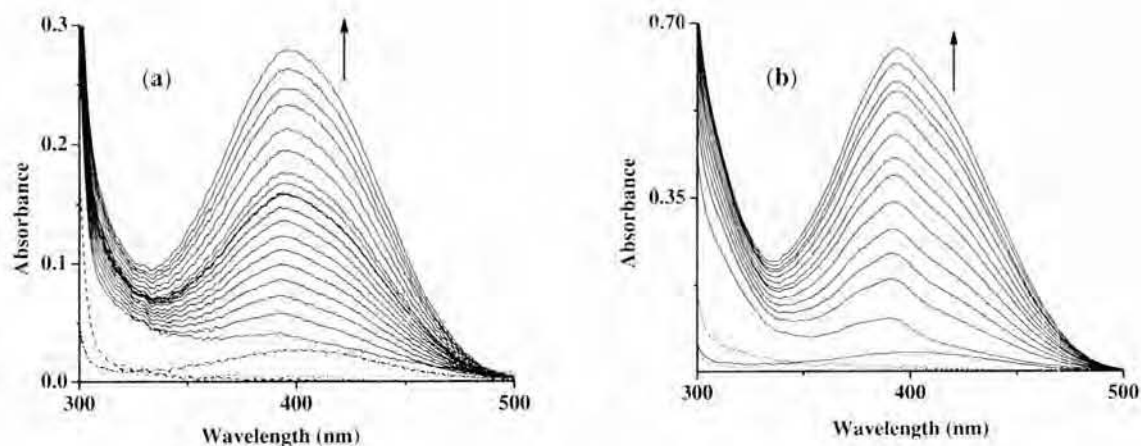


Fig. 3—Absorption spectral traces as a function of time (4 hrs duration) in the range 300–500 nm for the oxidative reaction of 3,5-DTBC by the Cu(II) complexes. [(a) **1** and (b) **2**, at the mole ratio of 3,5-DTBC : complex as 50:1].

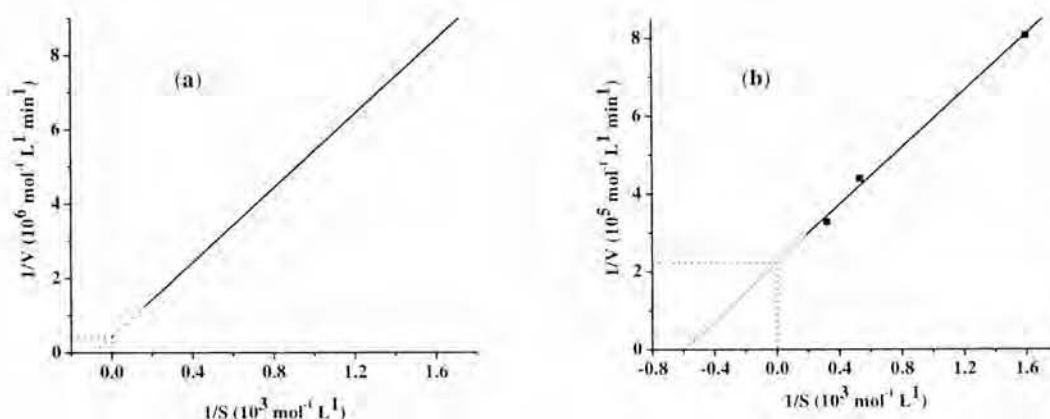


Fig. 4—Lineweaver-Burk plots ($1/V$ versus $1/S$) for (a) **1** and (b) **2**, for the oxidation of 3, 5-DTBC measured at the ratios of the complex : 3,5-DTBC of 1:50, 1:20 and 1:10.

Table 1—Kinetic parameters obtained from Lineweaver-Burk plot for the oxidation of 3, 5-DTBC by **1** and **2**

Complex	k_{cat} (h^{-1})	V_{max} ($10^6 M \text{ min}^{-1}$)	K_M (mM)	K (10^{-3} min^{-1})
1	7.7	2.0	11.6	5.67
2	18.0	4.8	1.8	35.7

This study clearly demonstrates the spectral and magnetic data differences between the mono- and dinuclear copper complexes of calix[4]arene-1,3-diacid derivative and clearly elicits the better catecholase mimetic activity of the dinuclear one owing to its Cu_2O_2 core.

Acknowledgements

CPR acknowledges the financial support from the Department of Science and Technology(DST), New Delhi and the Council of Scientific and Industrial Research (CSIR), New Delhi. AA acknowledges the SRF fellowship from CSIR. We thank RSIC, CDRI Lucknow for Mass Spectral measurements.

References

- 1 Penalver M J, Hiner A N P, Rodríguez-Lopez J N, Garcia-Canovas F & Tudela J, *Biochim Biophys Acta*, 1579 (2002) 140.
- 2 Than R, Feldman A A & Krebs B, *Coord Chem Rev*, 182 (1999) 211.
- 3 Malachowski M R & Davidson M G, *Inorg Chim Acta*, 162 (1989) 199.
- 4 Malachowski M R, Tomlinson L J, Davidson M G & Hall M J, *J Coord Chem*, 25 (1992) 171.
- 5 Reim J & Krebs B, *J Chem Soc, Dalton Trans*, (1997) 3793.
- 6 Malachowski M R, Carden J, Davison M G, Driessen W L & Reedijk J, *Inorg Chim Acta*, 257 (1997) 59.
- 7 Solomon E I, Sundaram V M & Machonkin T E, *Chem Rev*, 96 (1996) 2563.
- 8 Dey M, Rao C P & Gouinnie P, *Inorg Chem Commun*, 8 (2005) 998.
- 9 Rao P V, Rao C P, Kolehmainen E, Wegelius E K & Rissanen K, *Chem Lett*, 10 (2001) 1176.
- 10 Ali A, Salunke-Gawali S, Rao C P & Linares J, *Inorg Chem Commun*, 7 (2004) 1298.
- 11 Kumar A, Ali A & Rao C P, *J Photochem Photobiol A: Photochem*, 117 (2006) 164.
- 12 Deacon G B & Phillips R J, *Coord Chem Rev*, 33 (1980) 227 and references therein.
- 13 Dutta R L & Syamal A, *Elements of Magnetochemistry*, 2nd Edn. (Affiliated East-West Pvt. Ltd. Press New Delhi) 1993.
- 14 Bentiss F, Lagrene M, Mentre O, Conflant P, Vezin H, Wignacourt J P & Holt, E M, *Inorg Chem*, 43 (2004) 1865.
- 15 Kahn O, *Molecular Magnetism*, (VCH Publishers Inc, New York) 1993.
- 16 Chen Z N, Fu D G, Yu K B & Tang W X, *J Chem Soc Dalton Trans*, (1994) 1917.
- 17 Yang C-T, Vetrichelvan M, Yang, X, Moubaraki B, Murray K S & Vittal J J, *J Chem Soc Dalton Trans*, (2004) 113.
- 18 Selmezi K, Réglér M, Giorgi M & Speier G, *Coord Chem Rev*, 245 (2003) 191 and references therein.
- 19 Baruah P & Swain T, *J Sci Food Agric*, 10 (1959) 125.